Pergamon

Journal of Structural Geology, Vol. 17, No. 3, pp. 435 to 446, 1995
Elsevier Science Ltd
Printed in Great Britain
0191-8141/95 $9.50 + 0.00

0191-8141(94)00066-2

High and low density fluids in a quartz vein from the Irish Variscides

PATRICK A. MEERE

Department of Earth Science, The University, Leeds LS2 9JT, U.K.

(*Received* 2 *November* 1993; *accepted in revised form* 5 *May* 1994)

Abstract—Combined microstructural and fluid inclusion studies on a multiple quartz vein from the Irish Variscides reveal a kinematic history consisting of three separate, dynamically distinct, extensional opening events. The first of these is characterized by trapped fluid at densities of 0.87–0.98 g cm^{-3}, indicative of pressures approximating the estimated lithostatic load, while fluid densities associated with the following two events (0.76–0.91 g cm^{-3}) clearly indicate sub-lithostatic fluid pressures. The combined evidence suggests that these later two opening events were extensional fractures occurring well below the critical depth for tensional σ_3 (least effective principal stress). It is argued here that the preservation of such low density fluids, in an environment that conventionally requires supra-lithostatic fluid pressures for hydraulic failure, is due to (i) the influence of a pre-existing material anisotropy in the rock that would result in hybrid extensional failure, (ii) the effect of stress heterogeneities associated with the development of crude boudins in the vein.

INTRODUCTION

The last four decades have seen an increased understanding in the role of fluid behaviour and composition in deformational processes in low grade metamorphic terrains. The importance of elevated fluid pressures in brittle failure in the earth's crust was first recognized by Hubbert & Rubey (1959) in their model for regional overthrusting. High fluid pressure associated with tensile (Mode I) fracturing was subsequently invoked to account for the development of such fractures below a restricting critical depth controlled by the strength of the rock overburden. Assuming normal hydrostatic gradients, this critical depth (z), below which σ_3 (least effective principal stress) must be compressive, was given by Hubbert (1951) as

$$z = \sigma_1/[(\mu_s - \mu_w)g(1 - \varepsilon)] \quad (1)$$

where σ_1 is maximum effective stress, μ_s and μ_w mineral and water densities and ε rock porosity. The value of z has a range in the order of 10^2 m for consolidated sediments to several km for the strongest crystalline rock (Hubbert 1951). The implication therefore is that elevated fluid pressure is the only means of opening tensile cracks below this critical depth by pushing σ_3 into the tensile field and to a value higher than the tensile strength of the rock, i.e.

$$(S_3 - P_f) < T \quad (2)$$

where S_3 is the least principal stress, P_f fluid pressure and T the tensile strength of the rock (Hubbert & Willis 1957). Secor (1965) demonstrated that there was no limiting depth in the crust at which this mechanism could not operate. The above also assumes the second requirement for tensile failure, based on the interaction of stress circles and the Griffith failure envelope

$$(\sigma_1 - \sigma_3) < 4T \quad (3)$$

is satisfied.

This need for the elevated (supra-hydrostatic) fluid pressures associated with hydraulic failure as the only means of opening extensional fractures at depth has become almost universally accepted. However, recent studies on the densities of fluids trapped in minerals healing such fractures, have brought this assumption into some doubt. It is becoming increasingly evident that these fluids are often trapped significantly below lithostatic fluid pressures and contradict the assumption of hydraulic fracturing (e.g. Parry & Bruhn 1986, Vrolijk 1987, Grant *et al.* 1990, Foreman & Dunne 1991, O'Hara & Haak 1992). Foreman & Dunne (1991), in examining bedding-normal calcite veins from the southern Appalachian foreland, described fluid densities indicative of $P_f < P_l$ (P_l lithostatic pressure) in inclusions trapped at depths well below the critical depth for the limestone host lithology. Similarly, O'Hara & Haak (1992) found low density fluids in bedding-parallel deformed quartz veins associated with the Rector Branch thrust, North Carolina, that yielded trapping conditions up to 2 kbars below the calculated lithostatic pressure. In this case, however, they argue that post-trapping perturbations (i.e. leakage) and re-equilibration at lower densities was responsible for the low trapping pressure estimates. While this may sometimes be the case, it is striking that of the six veins examined, five gave pressure estimates that ranged well below the calculated lithostatic pressure. Meere (1992), in a study of syn-tectonic quartz veins in the Irish Variscides, noted a distinct bimodality in inter-vein fluid densities, with one group opening under estimated lithostatic fluid pressure conditions and a second group associated with hydrostatic fluid pressures. The pressure

difference between the two vein groups was again estimated to be up to 2 kbars. To date, little work has been carried out on possible mechanisms for trapping low density fluids at depth. Vrolijk (1987) accounted for low density inclusions in a syn-tectonic quartz vein from the Alaskan Kodiak accretionary complex by relating them to pockets of fluid trapped in irregularities along the fluid/rock interface after vein collapse. The irregularity of such a surface implies considerable spatial variation in fluid density throughout a single vein which is quite often not apparent (O'Hara & Haak 1992, Meere 1992).

This paper examines the possibility of alternative dynamic models for coaxial extensional fractures at depth. This study will initially present further evidence for the preservation of low density fluids in a multiple extensional quartz vein from the western Irish Variscides and then attempt to present some alternative models to account for the presence of these fluids.

GEOLOGICAL SETTING

The vein under investigation comes from the Mountain Mine in the Allihies copper district, at the western end of the Beara Peninsula, SW Ireland. Sheridan (1964) demonstrated the detailed relationship of geological structure to copper mineralization in the mine, postulating that barren veins, like the example in this study, were Variscan structures while the main quartz lodes were hydrothermal in origin and post-date the main Variscan folding/faulting event. Halliday & Mitchell (1983) confirmed this, obtaining younger, post-Variscan K–Ar dates (*c.* 290 Ma) for the lodes and older, Variscan (307–331 Ma) dates for the barren structures.

The Allihies area is located on the northern limb of the Beara anticlinorium at the western extremity of the Irish Variscan fold/thrust belt (Coe & Selwood 1963). The Late Palaeozoic tectonic evolution of this area commenced with Mid-Devonian crustal extension and the deposition of alluvial sheet flood sediments in a large E–W-trending half-graben, the Munster Basin (Williams *et al.* 1989). The Late Devonian saw the superimposition of the marine South Munster Basin on the southern part of the earlier structure.

Regional extensional tectonics were terminated at the end of the Carboniferous with the onset of Variscan compressional deformation. An early stage of layer parallel shortening preceded buckling and reactivation of basin controlling faults (Sanderson 1984, Cooper *et al.* 1986, Price & Todd 1988, Meere 1992). Thermal maturation studies indicate a peak temperature of metamorphism in the range 250–325°C (Price 1986, Clayton 1989, Clayton *et al.* 1989, Jones 1992, Meere 1992). Combining measured and inferred overlying stratigraphic thicknesses for the Allihies area yields an estimate of Upper Devonian/Carboniferous overburden thickness of 8–10 km for western Beara (Naylor *et al.* 1981, Graham 1983). This estimate includes a maximum composite thickness of Namurian and Westphalian strata in Ireland and western Britain of *ca.* 5 km (Clayton 1989).

The quartz vein investigated in this study is located in the area of the Mountain Mine east–west copper lode, in the hinge zone of a moderately plunging (30–40°W) anticline (wavelength ≈40 m) with concordant minor folding. The host lithology consists of a pale grey–green coarse-grained siltstone. The vein, which strikes 071° and dips 60°N, transects the fold axial trace (082°) and the single cleavage fabric which strikes 044° and dips 65°N. The thickness of the vein ranges from 10 to 20 cm and it has a surface trace of *c.* 30 m. Its overall axial planar orientation and absence of mineralization indicate that it is an essentially Variscan structure belonging to the older (307–331 Ma.) K–Ar age category (Haliday & Mitchell 1983). It is predominantly of quartz with no sulphide mineralization, but thin cross-cutting seams of chlorite do occur. Finely disseminated white mica is present in chlorite aggregates along these seams.

METHODOLOGY

Vein microstructure was investigated using transmitted light and S.E.M. microscopy on standard petrographic thin sections and resin block mounts, respectively. The cathodoluminescence (CL) detector in the pseudochannelling operating mode of the SEM was utilized in an attempt to characterize quartz growth zoning and microfracturing (see Lloyd in press a,b for experimental details). While CL in quartz is thought to be associated with crystal impurities and/or defects, it is well known that the crystal growth temperature is an important control on the intensity of luminescence. Sedimentary authigenic quartz, for example, appears much darker than metamorphic quartz (Marshall 1988). CL is also useful in identifying micro-fracture patterns not readily visible using normal optical microscopy (Sprunt & Nur 1979, Blenkinsop & Rutter 1986, Kanaori 1986, Shimamoto *et al.* 1991, Lloyd & Knipe 1992).

A doubly polished oriented thick section (200 μm) was prepared for fluid inclusion studies. Fluid inclusion plane (FIP) orientation data were recorded following the method of Boullier & Robert (1992), which involves measurement of the azimuth, projection width and depth of individual planes on a petrological microscope with a calibrated micrometric focusing screw. Fluid inclusion plane (FIP) orientations are a useful aid in establishing the orientation and chronology of specific stress regimes during the tectonic evolution of a given rock mass (Lespinasse & Pecher 1986, Cathelineau *et al.* 1990, Lespinasse & Cathelineau 1990, Lespinasse *et al.* 1991, Boullier & Robert 1992). Microthermometric investigations were carried out utilizing a Linkam TH600 heating/freezing stage, calibrated for the full temperature range in this study. Repeated measurements on an individual inclusion during a heating run yielded an accuracy range of ±0.3°C. Repeated calibration during the course of the study revealed no significant drift.

Fluid inclusions were all aqueous and bi-phase (liquid/

vapour), ranging in size from 1–15 μm. The small size of secondary inclusions (1–3 μm) prevented a detailed microthermometric study of planes, all data coming from primary and possibly pseudo-secondary structures.

RESULTS

Microstructure

The gross internal microstructure is dominated by at least four distinct cross-cutting generations of quartz (Fig. 1, Zone 4 not shown). The earliest quartz growth is deformed to a highly strained micro-breccia (Zone 1), which is cut by well preserved euhedral material (Zone 2). Euhedral quartz is in turn cross-cut by fibrous quartz (Zone 3) and there is a final generation of clear euhedral quartz (Zone 4). The fact that three of these zones (Zones 2–4) represent quartz growing on a pre-existing, virtually pure, quartz substrate leads to a marked absence of solid inclusion planes typical of crack seal-opening (Ramsay 1980). However, grain morphology and microstructure of quartz from the differing zones can still yield valuable insights on the complete kinematic history of the vein (Fisher & Brantley 1992).

Zone 1. The first phase of quartz growth, a micro-breccia, is characterized by 100–200 μm isolated grains preserved in a matrix of finer-grained quartz and insolubles. The finer-grained material exhibits well developed serrated grain contacts and sub-grain development, clear evidence of dynamic recrystallization (Fig. 2c). The grains often seem to be basal sections in slides cut orthogonal to the vein wall. A dense, anastomosing network of insolubles runs parallel to the vein wall indicating that σ_1 was sub-perpendicular to the wall during the compressive event responsible for the observed micro-brecciation. These seams are truncated by all later quartz growth events. Selvages of very fine-grained quartz are interpretated as laminae of the host lithology siltstone incorporated into the vein during this early opening event. The overall high insoluble content preserved in this zone points to significant post-brecciation diffusive mass transfer (Knipe 1989). Intra-granular plasticity is not important.

Zone 2. The second phase of quartz growth is composed of large (600–900 μm) well preserved euhedral crystals, with a preferred growth direction orthogonal to the vein wall and vein parallel fractures in which they occur. The euhedral nature of quartz growth suggests an uninterrupted growth history with, if necessary, individual crack increments outpacing quartz growth and maintaining a fluid filled cavity throughout this period of vein opening. This manner of quartz growth does not allow displacement paths to be deduced as the quartz will simply grow out from the walls.

Zone 3. Quartz from this zone clearly cross-cuts the two previous zones and is composed of straight, well developed fibres 100–250 μm in width and up to 1500 μm in length. They form sub-parallel bifurcating sheets that run at high angles to the vein walls. Individual fibre axes run normal to the sheet wall and parallel to the original vein wall and its overall dip. These fibres seem to maintain constant width for most of their length, probably reflecting the relatively homogeneous quartz substrate from which they grew and the complete healing of individual co-axial opening increments. The influence of host quartz grain size is especially highlighted when fibre width dramatically increases passing from Zone 1 (micro-breccia) to Zone 2 (euhedral) substrate. There is no evidence of a shear component to the opening history. Dynamically therefore, this stage of opening is characterized by the σ_3 axis running parallel to the overall vein dip.

Zone 4. This final stage of quartz growth occupies pre-existing cavities and irregularities throughout the vein. In contrast to earlier zones, the quartz is relatively clear of impurities and small fluid inclusions. Grains are roughly equidimensional in aspect. Quantitatively this quartz is not significant, making up less than 2% of the total vein quartz.

Finally a number of late-stage, isolated chlorite/white mica seams that are related to the post-Variscan copper mineralization event cross-cut all of the above quartz zones.

Cathodoluminescence studies

The first three quartz growth zones were examined in the CL operating mode of the S.E.M. (Kanaori 1986, Shimamoto *et al.* 1991).

The larger isolated grains of the Zone 1 micro-breccia exhibit well developed, undisturbed growth zones (Fig. 2a). There is no obvious systematic fracture overprint except for a number of isolated intra-granular fractures running sub-perpendicular to the vein wall. The absence of systematic fracturing is probably due to the mechanically heterogeneous nature of the strained quartz in the micro-breccia.

The images of Zone 2 euhedral quartz also reveal strongly luminescent crystals with well developed, undisturbed growth zoning similar to that in Zone 1. While undulose extinction indicates some intracrystalline plastic deformation, the predominant deformation feature in this zone, as revealed by CL studies, is a set of anastomosing inter-granular fractures running sub-perpendicular to the vein wall (Fig. 2b). These fractures are clearly defined by secondary infill of darker, dull grey luminescing quartz. Zone 3 fibrous quartz is virtually non-luminescent, appearing dark grey and without contrast. The scarcity of Zone 4 quartz prevented detailed investigations of this material.

Fluid inclusion planes

The fluid inclusion plane data were surprisingly systematic from a vein with such a complex opening history

(Fig. 3). The observed pattern in each of the quartz phases allows a fracture history for these healed cracks to be deduced, with each new growth phase recording subsequent dynamic events. It is also quite evident that when plane orientations are dynamically compatible with conditions for host quartz growth, inclusions forming these planes are in fact pseudosecondary and trapped during this primary growth phase. Compositionally the inclusions making up these planes are liquid-rich aqueous biphase inclusions ranging in size from 1–3 μm. It is convenient to start with the latest generation and retrace the chronology of quartz growth to the earliest opening event.

The FIP pattern in Zone 4 quartz is completely dominated by a set of planes running orthogonal to both the vein wall and overall dip (Set III). Individual planes are dominantly intra-granular in nature and presumably pseudosecondary in origin, being compatible with the dynamic regime for fibrous (Zone 3) quartz growth. The presence of this set in Zone 4 suggests that this quartz grew synchronous to or at least under the same stress conditions as Zone 3, i.e. σ_3 sub-parallel to the vein dip.

The FIP data from Zone 3 are clearly compatible with the dynamic conditions for the opening event associated with this generation of quartz growth, being oriented orthogonal to fibre long axes. This set of healed fractures is seen to dominate all quartz generations in the vein, illustrating the dominance of this opening event.

The FIP pattern in Zone 2, while also recording the late sub-vertical opening event (Set III), has a set of planes running parallel to the vein wall (Set II), possibly reflecting the dynamic conditions for Zone 2 quartz growth, i.e. σ_3 orthogonal to the vein wall. Again this latter set is probably pseudosecondary in origin.

The dominance of the vertical opening event during Zones 3 and 4 quartz growth is again evident from the FIP pattern observed in Zone 1 quartz (i.e. the presence of Set III healed fractures). In addition to this healed fracture set, a smaller set running at right angles to the vein wall and dip is also evident (Set I). This early set of planes probably represents fracturing during the main compressive event that produced micro-brecciation in Zone 1.

Microthermometry

Primary inclusions from the four quartz zones were studied utilizing the standard techniques of microthermometry (Shepherd *et al.* 1985) in an attempt to characterize fluid density and composition for each of the main trapping events. While the study of inclusions in vein quartz has a number of distinct limitations due for example to the influence of inclusion leakage on fluid density (Roedder 1984), it is possible, in interpreting the data, to draw some reasonable conclusions on the trapping conditions and nature of the fluid under investigation. Highly strained quartz crystals were avoided where possible in an attempt to minimize the effects of post-trapping perturbations on density data. The 10–15 μm size of the majority of the inclusions prevented detailed freezing studies. Figure 4(a) shows that freezing point depression data for Zone 1 quartz lie between −8 and −20°C while those from Zones 2 to 4 lie within a range of 0° to −8°C. These results correspond to 10–22 wt.% and 0–10 wt.% NaCl equivalent, respectively (Potter & Brown 1977).

The bulk homogenization temperature data similarly indicate a marked difference between data from the Zone 1 micro-breccia (130–210°C) and those from Zones 2 to 4 (190–330°C) (Fig. 4b). These results correspond to fluid densities of 0.87–0.98 g cm^{-3} and 0.76–0.91 g cm^{-3}, respectively (Potter & Brown 1977). Leakage and the subsequent re-equilibration of fluid at lower densities does not seem to be important, as the micro-breccia, which would have been most susceptible to such a phenomenon, has preserved the highest density fluids. Combining these data with estimated salinities for each of the four quartz zones and plotting the full range of *P–T* conditions for the two fluid types (shaded areas), utilizing the FLINCOR program (Brown 1990), graphically illustrates this striking difference in fluid density (Fig. 5).

Assuming a full temperature range of 250–325°C for peak Variscan metamorphism (Clayton 1989, Clayton *et al.* 1989, Jones 1992, Meere 1992), a trapping pressure difference of up to 2 kbars existed between the two groups of fluid inclusion densities. This also assumes that fluid temperatures were not significantly different from host rock temperatures. It has been shown from oxygen isotope studies that there is little evidence of significant fluid flux and infiltration of externally derived fluids during low grade segregation vein development similar to that in the Irish Variscides (Gregory 1993, Slater *et al.* in press). Also, there is no evidence of metasomatic effects on the wall rock expected from influx of 'hot' hydrothermal fluids.

This gap in fluid pressure may be somewhat narrowed if a significantly lower trapping temperature is assumed for Zone 1 inclusions. However, the fact that Zone 1 quartz luminesces under CL and exhibits well developed growth zoning indicates that this quartz also grew under low grade metamorphic conditions (Marshall 1988, p. 69) and implies that the observed difference in density truly reflects different trapping fluid pressures.

The estimated drop in fluid pressure in Zones 2, 3 and 4 may be due to isothermal uplift and trapping under decreased lithostatic loads. This would require that temperatures of *ca.* 300°C should remain relatively constant during uplift that brings rocks from depths of 8–10 km to within 2–3 km of the surface. While rapid uplift can produce nearly isothermal trajectories (Koons 1987), the rates of uplift required (*ca.* 10 mm a^{-1}) are usually associated with orogenic hinterlands and areas proximal to crustal scale faults and are unlikely in a foreland fold belt. The tectonic setting of the Irish Variscides, where layer parallel shortening and buckling were the dominant crustal shortening mechanisms, is unlikely therefore to produce the necessary rates of uplift.

If normal continental geothermobaric gradients for

Fig. 1. Photomicrograph of section cut normal to the vein wall showing three main quartz zones (1–3).

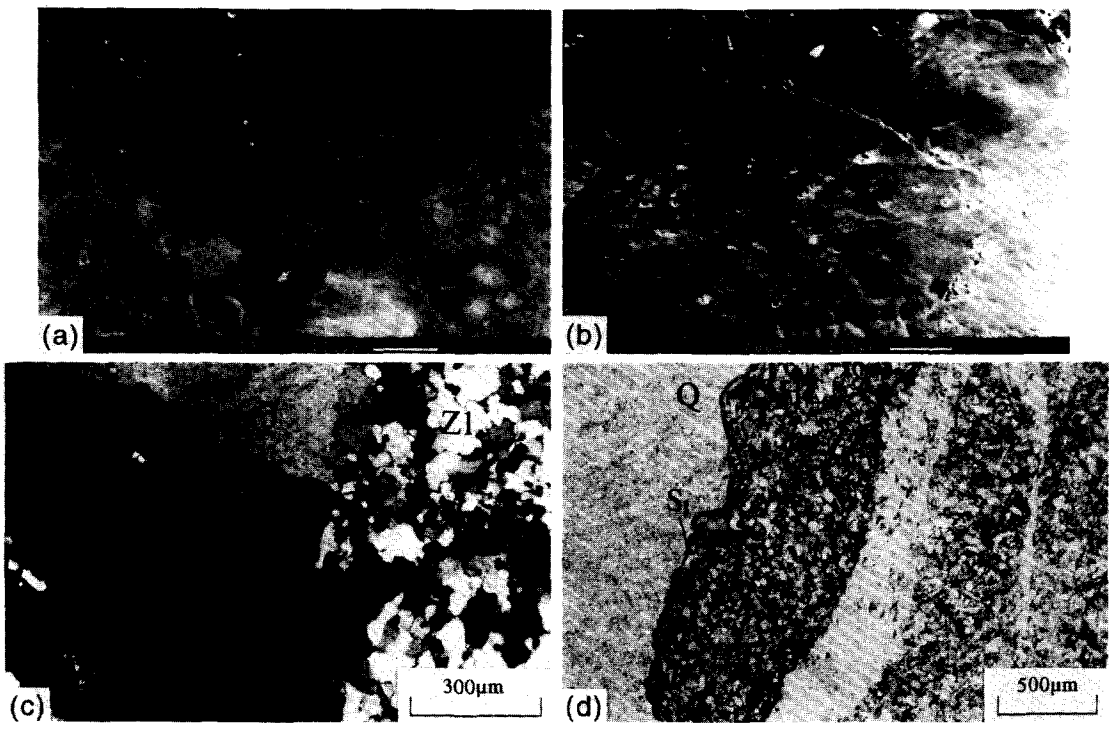

Fig. 2. (a) Cathodoluminescence scanning electron microscope image of Zone 1 quartz. Note well developed growth zoning. (b) Similar image of Zone 2 quartz exhibiting well developed growth zoning and a transgranular systematic fracture set. (c) Zone 1 (Z1)/Zone 2 (Z2) contact with Zone 1 grains showing clear evidence of dynamic recrystallization. (d) Photomicrograph of host lithology (HL)/vein quartz (Q) contact illustrating exploitation of cleavage solution seams (S_1) during the vein opening event.

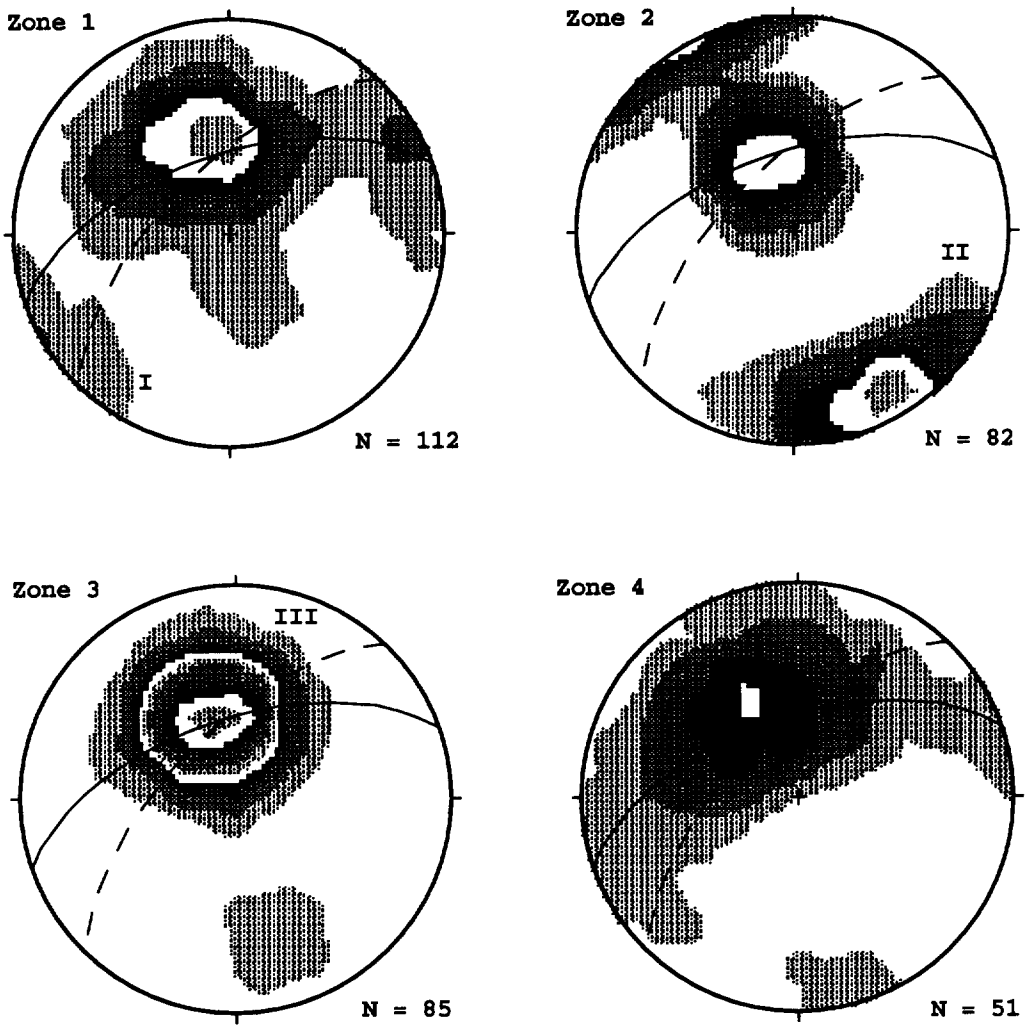

Fig. 3. Contoured plots (interval: 2.0 sigma) of poles to fluid inclusion planes (FIP) data (Sets I–III) for quartz Zones 1–4. Also plotted are great circles for the vein (solid) and cleavage (dashed) orientations. Contoured according to Kamb (1959).

lithostatic and hydrostatic conditions at 25°C km^{-1} are superimposed on the isochore plot in P–T space (Fig. 5), it is evident that Zone 1 quartz grew under conditions approximating lithostatic pressure (*ca.* 2000 bars). This pressure estimate is also compatible with Late Palaeozoic overburden thickness of 8–10 km (Naylor *et al.* 1981, Graham 1983). In contrast, quartz in the later three zones grew in fluid close to hydrostatic pressure conditions (*ca.* 800 bars), again assuming a normal geothermal gradient. Possible alternative models to account for this variation in fluid pressure will be discussed in the next section.

VEIN OPENING HISTORY AND DISCUSSION

The earliest phase of quartz growth (Zone 1) clearly pre-dates the main compressional deformation event recorded in the vein (Fig. 6a). Extensive microbrecciation of Zone 1 quartz is a result of a major phase of compression normal to the vein wall. The FIP data and preservation of euhedral grains suggest that the quartz originally grew in a simple Mode 1 fracture, possibly related to pre-Variscan extensional tectonics in the area (Fig. 6b). The preservation of high density fluids in Zone 1 quartz also suggests that normal hydrofracturing was the mechanism for this opening event, i.e. $P_f \approx P_l$ (Fig. 7a). Subsequent Variscan compression is presumed to have produced the observed microbrecciation. It is difficult to place this event in the overall compressional history of the area. However, the absence shear indicators, the high percentage of insolubles and the presence of other pressure solution features, suggests that it was linked to the early layer-parallel shortening event that was responsible for the main cleavage.

The timing of Zone 2 quartz growth is more problematic in that it is dynamically compatible equally with tangential longitudinal strain fracturing associated with Variscan folding, or with a post Variscan extension event (Fig. 6c). However, as this zone is clearly cross-cut by Zone 3 fibrous quartz which is related to vertical opening and presumably horizontal compression, it seems likely that Zone 2 opening is linked to early buckling stresses. On-going Variscan compression led to regional scale buckling and associated lower order folds after the main layer parallel shortening event.

The presence of a competent quartz vein in the rock

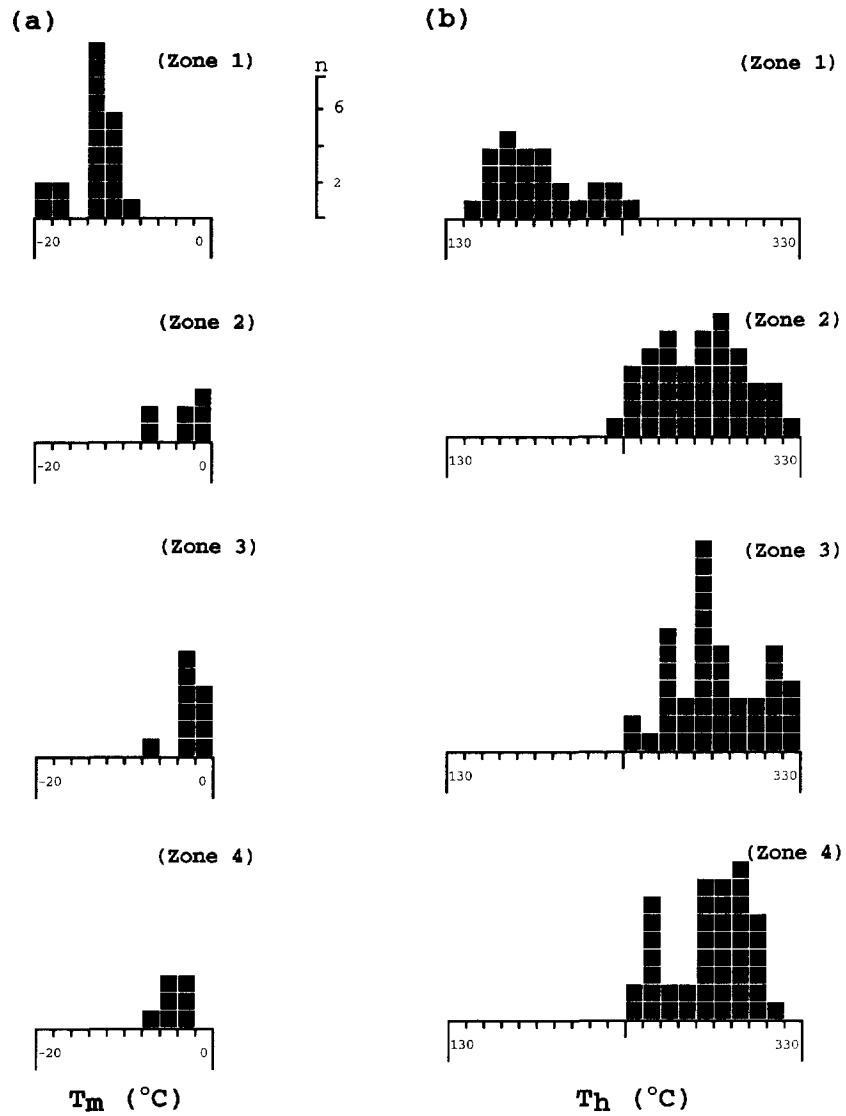

Fig. 4. (a) Final ice melting temperature data for quartz Zones 1–4. (b) Bulk homogenization temperature data for Zones 1–4.

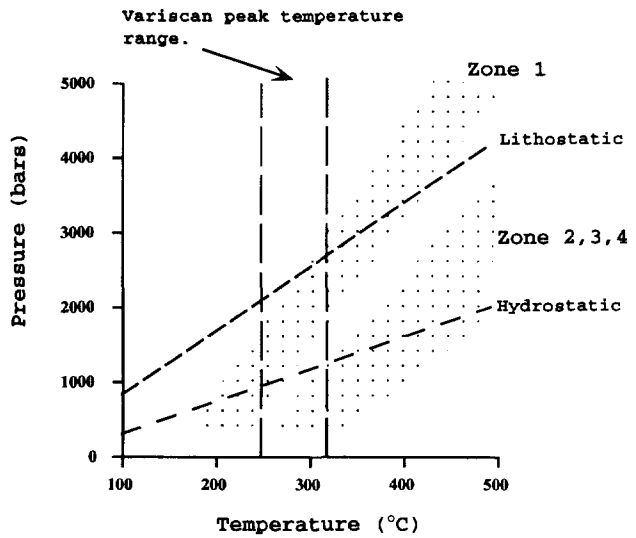

Fig. 5. Isochore envelopes for the full range of Zone 1 and Zones 2, 3 and 4 fluid densities. Peak Variscan temperature range along with geothermobaric gradients for hydrostatic and lithostatic conditions are also included. Geothermal gradient assumed to be 25°C km^{-1} and rock density 2.7 g cm^{-3}.

pile might have provided an ideal perturbation from which buckling could have been nucleated (Price & Cosgrove 1990). While a number of studies have investigated the interplay between fluid behaviour and faulting (Sibson 1985, 1988, 1989, 1993, Knipe *et al.* 1991, Knipe 1992, 1993), relatively little work has been carried out on the relationship of fluid behaviour to folding. Cosgrove (1993), utilizing the theoretical results of Summers (1979), postulated possible fluid migration paths during folding based on the evolution of internal (σ_i) and external (σ_e) mean stresses during fold amplification. Cosgrove's model predicts that fluids, while initially being drawn into the fold during the early stages of amplification, will subsequently be expelled at a critical fold amplitude and driven from the limbs to hinge zones. The hinge region is an area of considerable fracture permeability during folding. It is the site of numerous accommodation structures between mechanically incompatible layers and fractures related to tangential longitudinal stresses. These later structures can provide quite an efficient pathway for upwardly migrating fluids. Bending stress in the hinge region of a fold during

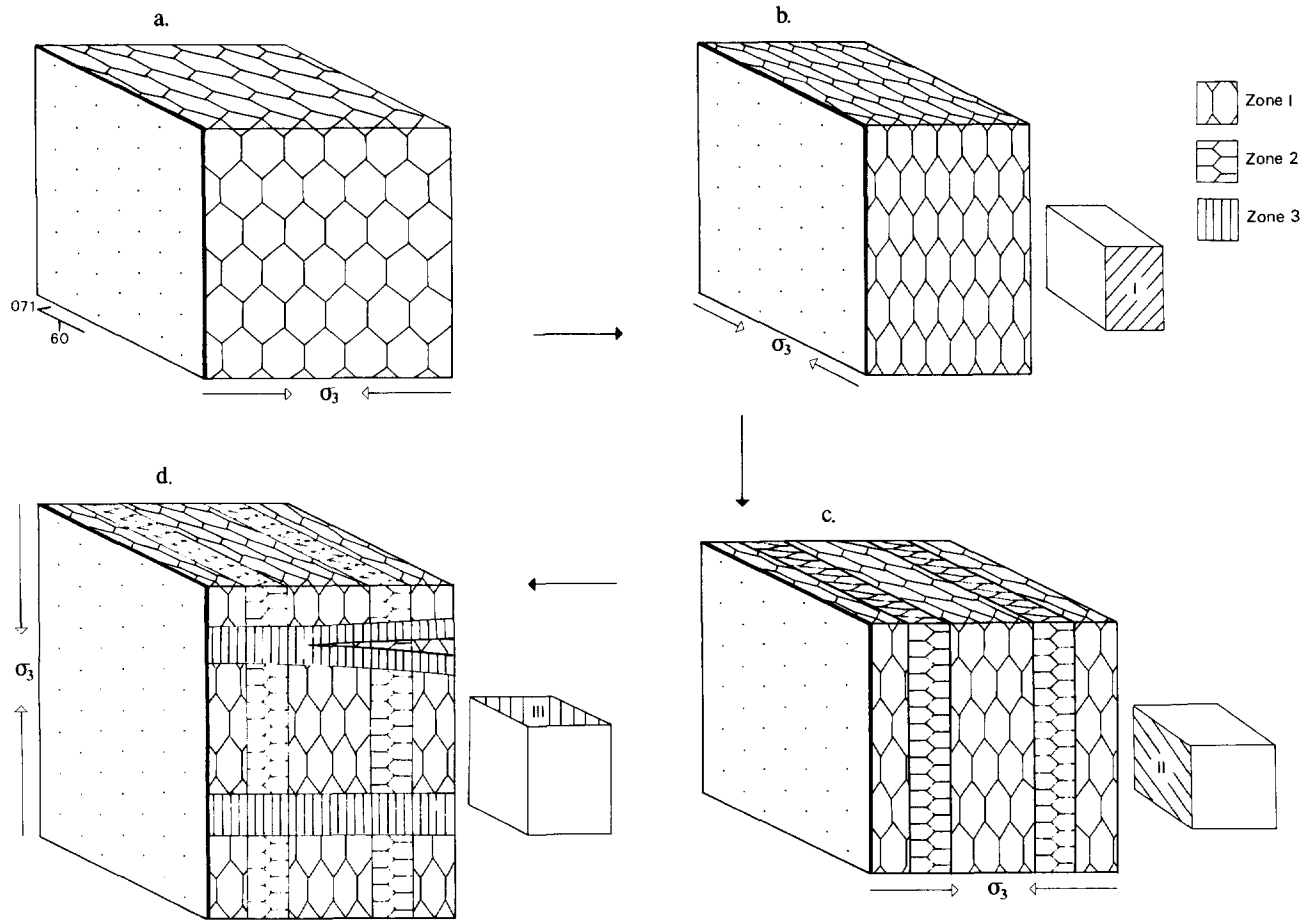

Fig. 6. Schematic representation of three main vein opening events: (a) first opening event with growth of Zone 1 quartz; (b) deformation of Zone 1 quartz and possible development of FIP Set I; (c) the second vein opening event, growth of Zone 2 euhedral quartz and development of FIP Set II; (d) final sub-vertical opening event, growth of Zone 3 fibrous quartz and development of FIP Set III.

amplification will result in local σ_3 acting parallel to the maximum far field principal compressive stress. Ongoing amplification will progressively lower this σ_3 value. Decreasing σ_3 and assuming that σ_1 is locally sub-vertical and equal to the lithostatic load will increase differential stress ($\sigma_1 - \sigma_3$) which should in turn produce compressional shear failure and not the extensional opening observed in Zone 2.

One possible explanation for extensional failure under these conditions might be the influence of a pre-existing anisotropy in the rock; i.e. the cleavage fabric. This increases the ratio of compressive to tensile strength of the rock and will significantly lower the trace of the failure envelope on a Mohr diagram (Fig. 7b) (Jaeger 1960, Donath 1961). In the present example, assuming a sub-vertical σ_1 axis, the angle between this axis and the anisotropy (θ) is quite low in the fold hinge region rendering it ideal for exploitation during failure. Decreasing σ_3 will therefore result in hybrid extensional failure along this anisotropy if 2θ is less than 45° and σ_3 is allowed to move into the tensile field before compressional shear failure. There is abundant field evidence in the Allihies Mine area of extensional veins exploiting cleavage. Figure 2(d), a photomicrograph taken from a vein section adjacent to and structurally similar to the vein under investigation, clearly illustrates this process on a microscopic scale. There is however a lower depth limit for hybrid failure under these conditions. It is evident from Fig. 7(b) that, for hybrid failure,

$$\Delta\sigma < 8T \tag{4}$$

where $\Delta\sigma$ is the effective differential stress (Price & Cosgrove 1990). If a typical tensile strength of 50 bars is assumed for these metasediments (Etheridge 1983), it follows that σ_1 cannot exceed 400 bars. Taking an estimated fluid pressure (P_f) of 800 bars gives a maximum S_1 value of 1200 bars ($S_1 = P_f + \sigma_1$) which is approximately equivalent to 4.5 km of overburden. Higher tensile strengths will lower this depth limit. The implication is that Zone 2 opening occurred after a significant amount of uplift and denudation. The vein's overall structural position on the northern limb of a regional anticlinorium would support this. It might also be possible that localized stress heterogeneities will reduce σ_1 to a value that is compatible with hybrid extension (see below). It is quite conceivable therefore that fluid pressures associated with hybrid extensional fracturing in these circumstances can be quite low and not the elevated pressures required for hydrofracturing. The trapping of low density fluid in Zone 2 quartz would seem to bear this out. Because of relatively low fold amplification strain rates, a relatively stable, low fluid

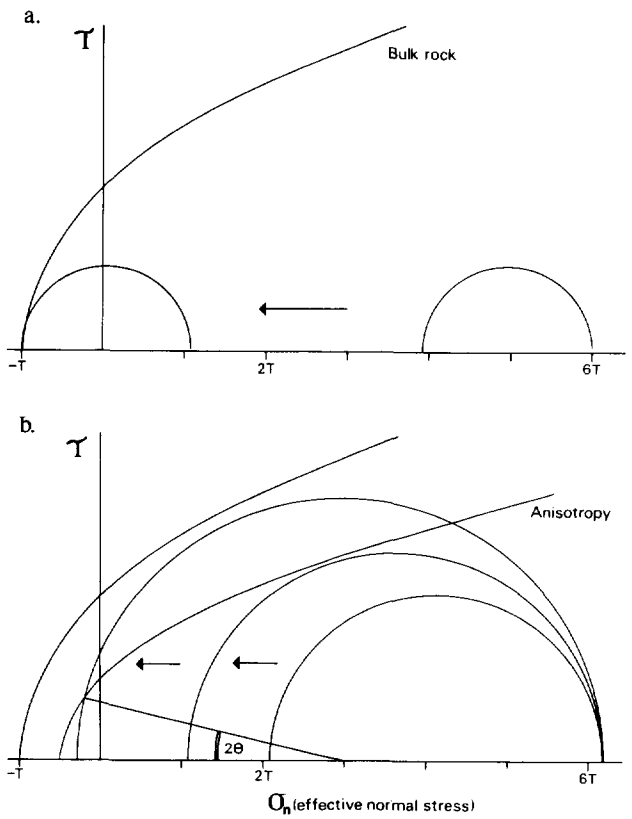

Fig. 7. Mohr diagram representation of failure conditions associated with (a) hydraulic failure in an isotropic rock, and (b) hybrid extension by keeping σ_1 fixed and lowering σ_3 in a rock with a material anisotropy ($2\theta < 45°$).

pressure, open fracture system to upper crustal levels is envisaged, accommodating upward expulsion of fluid related to fold amplification.

The final strain event related to Zone 3 and possibly Zone 4 quartz growth is characterized by vertical extension and the opening of sub-horizontal fractures (Fig. 6d). Fluid inclusion planes related to this opening event have overprinted all earlier phases of quartz growth. Its non-luminescence under CL suggests that this phase of quartz growth was at lower temperatures than previous generations. However, minimum trapping temperatures (230–330°C) indicate that the difference was not large. This drop in temperature is to be expected with progressive uplift and denudation.

Again the trapping of Zone 3 and 4 fluids at sub-lithostatic pressures requires some consideration. In this case σ_3 is clearly sub-vertical and equivalent to overburden lithostatic pressure, so it is a mechanical prerequisite at the point of failure that fluid pressures are greater than the lithostatic load. These conditions for hydraulic failure must have been achieved as the fibrous quartz textures clearly point to tensile failure. However, the continued opening may have been controlled by alternative mechanisms for maintaining an open, fluid filled crack at depth. Vrolijk (1987) accounted for trapping of low density, methane-rich fluids by envisaging the irregular growth of quartz along a fracture that would allow small pockets of low density fluid to be preserved after a fluid pressure drop and crack collapse. This mechanism of trapping does not, however, account for the consistency in fluid density data for Zones 2, 3 and 4. Scatter in fluid density reflecting elevated and reduced fluid pressures related to differing stages in quartz growth is clearly not evident in these quartz zones.

One possible explanation for the trapping of fluids in fibrous quartz at sub-lithostatic pressures may be the effect of stress heterogeneities associated with the development of crude boudins in the vein accompanying the cessation of fold amplification. Numerous experimental and theoretical studies have demonstrated that boudin neck regions are areas of markedly reduced mean and differential stress (Goguel 1948, Ramberg 1955, Voight 1965, Stephenson & Berner 1971, Stromgard 1973, Lloyd & Ferguson 1981, Oliver *et al.* 1990). This will allow local σ_3 to be pushed into the tensile stress field in a manner similar to that illustrated in Fig. 7(a). The boudin necks, in this case running parallel to the fold axis, are filled with Zone 3 fibrous quartz trapped at sub-lithostatic fluid pressures. The drop in mean stress in these zones would locally facilitate quartz precipitation (Walter & Helgeson 1977). The isolated nature of these stresses does not require an open fracture network to the surface to account for the preservation of low density fluids.

CONCLUSIONS

Combined microstructural and fluid inclusion studies have revealed the presence of fluids trapped in quartz under sub-lithostatic conditions at depth. This illustrates the need for alternative models to hydrofracturing to account for vein opening at these depths. It is argued in this case that the effect of material anisotropies and stress heterogeneities initiate failure and control the subsequent evolution of fractures. These mechanisms imply that tensile failure below the critical depth (z) is a consequence of far field compressional stress and not locally elevated fluid pressure. Widespread evidence for the preservation of sub-lithostatic fluids in veins might suggest that these and similar mechanisms are the rule rather than the exception.

Acknowledgements—The funding for this research was provided by an EC Human Capital & Mobility grant. I am grateful to Geoff Lloyd for instruction and helpful suggestions on use of the SEM and Bruce Yardley for reviewing an early draught of the manuscript.

REFERENCES

Blenkinsop, T. G. & Rutter, E. H. 1986. Cataclastic deformation of quartzite in the Moine thrust zone. *J. Struct. Geol.* **8**, 669–681.

Boullier, A.-M. & Robert, F. 1992. Palaeoseismic events recorded in Archaean gold–quartz vein networks, Val d'Or, Abitibi, Quebec, Canada. *J. Struct. Geol.* **14**, 1161–1179.

Brown, P. E. 1990. FLINCOR: a microcomputer program for the reduction and investigation of fluid inclusion data. *Am. Miner.* **74**, 1390–1393.

Cathelineau, M., Lespinasse, M., Bastoul, A., Bernard, C. & Leroy,

J. 1990. Fluid migration during contact metamorphism: the use of orientated fluid inclusion trails for a time/space reconstruction. *Mineralog. Mag.* **54**, 169–182.

Clayton, G. 1989. Vitrinite reflectance data from the Kinsale Harbour—Old Head of Kinsale area, southern Ireland, and its bearing on the interpretation of the Munster Basin. *J. geol. Soc. Lond.* **146**, 611–616.

Clayton, G., Haughey, N., Sevastopulo, G. D. & Burnett, R. D. 1989. Thermal maturation levels in the Devonian and Carboniferous rocks in Ireland. *Spec. Publ. geol. Surv. Ir.*

Clyne, M. A. & Potter, R. W. 1977. Freezing point depression of synthetic brines (abstr.) *Geol. Soc. Am. Abstr. Prog.* **9**, 930.

Coe, K. & Selwood, E. B. 1963. The stratigraphy and structure of part of the Beara Peninsula, Co. Cork. *Proc. R. Ir. Acad.* **63B**, 33–59.

Cooper, M. A., Collins, D., Ford, M., Murphy, F. X., Trayner, P. M. & O'Sullivan, M. 1986. Structural evolution of the Irish Variscides. *J. geol. Soc. Lond.* **143**, 53–61.

Cosgrove, J. W. 1993. The interplay between fluids and thrusts during the deformation of a sedimentary succession. *J. Struct. Geol.* **15**, 491–500.

Donath, F. A. 1961. Experimental study of shear failure in anisotropic rocks. *Bull. geol. Soc. Am.* **72**, 985–990.

Etheridge, M. A. 1983. Differential stress magnitudes during regional deformation and metamorphism: Upper bound imposed by tensile fracturing. *Geology* **11**, 231–234.

Fisher, D. M. & Brantly, S. L. 1992. Models of quartz overgrowth and vein formation: deformation and episodic fluid flow in an ancient subduction zone. *J. geophys. Res.* **97**, 20,043–20,061.

Foreman, J. L. & Dunne, W. M. 1991. Conditions of vein formation in the southern Appalachians foreland: constraints from vein geometries and fluid inclusions. *J. Struct. Geol.* **13**, 1173–1183.

Goguel, J. 1948. Introduction a l'étude méchaniques des déformations de l'écorce terèstre, 2nd edition, Paris, France. *Mém. Serv. Carte géol. dét. Fr.*

Graham, J. R. 1983. Analysis of the Upper Devonian Munster Basin, an example of a fluvial distributary system. In: *Modern and Ancient Fluvial Systems* (edited by Collinson, J. D. & Lewin, J.). *Spec. Publ. Int. Ass. Sedimentol.* **6**, 473–483.

Grant, N. T., Banks, D. A., McCaig, A. M. & Yardley, B. W. D. 1990. Chemistry, source, and behaviour of fluids involved in Alpine thrusting of the central Pyrenees. *J. geophys. Res.* **95**, 9123–9131.

Gregory, R. T. 1993. Oxygen isotope systematics of coexisting veins and wall rocks from the Otago Schist, South Island, New Zealand. *Geol. Soc. Am. Abstr. Prog.* **25**, 78.

Halliday, A. N. & Mitchell, J. G. 1983. K–Ar ages of clay concentrates from Irish orebodies and their bearing on the timing of mineralisation. *Trans. R. Soc. Edinb.: Earth Sci.* **74**, 1–14.

Hubbert, M. K. 1951. Mechanical basis for certain familiar geologic structures. *Bull. geol. Soc. Am.* **62**, 355–372.

Hubbert, M. K. & Willis, D. G. 1957. Mechanics of hydraulic fracturing. *Trans. A.I.M.E.* **210**, 153–168

Hubbert, M. K. & Rubey, W. W. 1959. Role of fluid pressure in mechanics of over-thrust faulting, Part 1, Mechanics of fluid-filled porous solids and its application to overthrust faulting. *Bull. geol. Soc. Am.* **70**, 115–166.

Jaeger, J. C. 1960. Shear failure in anisotropic rocks. *Geol. Mag.* **97**, 65–72.

Jones, G. L. 1992. Irish Carboniferous conodonts record maturation levels and the influence of tectonism, igneous activity and mineralization. *Terra Nova* **4**, 238–244.

Kamb, W. B. 1959. Ice petrofabric observations from Blue Glacier, Washington, in relation to theory and experiment. *J. geophys. Res.* **64**, 1891–1909.

Kanaori, Y. 1986. A SEM cathodoluminescence study of quartz in mildly deformed granite from the region of the Atotsugawa fault, central Japan. *Tectonophysics* **131**, 133–146.

Knipe, R. J. 1989. Deformation mechanisms: recognition from natural tectonites. *J. Struct. Geol.* **11**, 127–146.

Knipe, R. J. 1992. Faulting processes and fault seal. In: *Structural and Tectonic Modeling and Its Application To Petroleum Geology* (edited by R. M. Larsden *et al.*). *Spec. Publ. NPF* **1**, 325–343.

Knipe, R. J. 1993. Faulting processes, fluid flow and the evolution of reservoir compartments. *Geofluids 1993 Extended Abstracts*, 134–136.

Knipe, R. J., Agar, S. M. & Prior, D. J. 1991. The microstructural evolution of fluid flow paths in semi-lithified sediments from subduction complexes. *Phil. Trans. R. Soc. A* **335**, 261–273.

Koons, P. O. 1987. Some thermal and mechanical consequences of rapid uplift: an example from the Southern Alps, New Zealand. *Earth Planet. Sci. Lett.* **86**, 307–319.

Lespinasse, M. & Pecher, A. 1986. Microfracturing and regional stress field: a study of the preferred orientations of fluid inclusion planes in a granite from the Massif Central, France. *J. Struct. Geol.* **8**, 169–180.

Lespinasse, M. & Cathelineau, M. 1990. Fluid percolations in a fault zone. A study of fluid inclusion planes (FIP). *Tectonophysics* **184**, 173–187.

Lespinasse, M., Cathelineau, M. & Poty, B. 1991. Time space reconstruction of fluid percolation in fault systems: the use of fluid inclusion planes (FIP). *Proc. 25th SGA anniv. Nancy*, A. A. Balkema Publ., 468–495.

Lloyd, G. E. In press a. SEM electron channelling. In: *Procedures in Electron Microscopy* (edited by A. J. Wilson). Wiley & Sons, New York.

Lloyd, G. E. In press b. An appreciation of the SEM electron channelling technique for microstructural analysis of geological materials. In: *Textures of Geological Materials* (edited by Bunge, H.-J. & Weber, K.). German Society of Materials Science.

Lloyd, G. E. & Ferguson, C. C. 1981. Boudinage structure: some interpretations based on elastic–plastic finite element simulations. *J. Struct. Geol.* **3**, 117–128.

Lloyd, G. E. & Knipe, R. J. 1992. Deformation mechanisms accommodating faulting of quartzite under upper crustal conditions. *J. Struct. Geol.* **14**, 127–143.

Marshall, D. J. 1988. *Cathodoluminescence of Geological Materials*. Unwin Hyman, Boston.

Meere, P. A. 1992. Structural and metamorphic studies of the Irish Variscides from the Killarney–Baltimore transect, southwest Ireland. Unpublished Ph.D. thesis, National University of Ireland.

Naylor, D., Sevastopulo, G. D., Sleeman, A. G. & Reilly, T. A. 1981. The Variscan fold belt in Ireland. *Geol. Mijnb.* **60**, 49–66.

O'Hara, K. & Haak, A. 1992. A fluid inclusion study of fluid pressure and salinity variations in the footwall of the Rector Branch thrust, North Carolina, U.S.A. *J. Struct. Geol.* **14**, 579–589.

Oliver, N. H. S., Valenta, R. K. & Wall, V. J. 1990. The effect of heterogeneous stress and strain on metamorphic fluid flow, Mary Kathleen, Australia, and a model for large-scale fluid circulation. *J. metamorphic Geol.* **8**, 311–331.

Parry, W. T. & Bruhn, R. L. 1986. Pore fluids and seismogenic characteristics of fault rock at depth on the Wasatch fault, Utah. *J. geophys. Res.* **91**, 730–740.

Potter, R. W. & Brown, D. L. 1977. The volumetric properties of aqueous sodium chloride solutions from 0°C to 500°C. *Bull. U.S. geol. Surv.* **1421-C**.

Potter, R. W., Clynne, M. A. & Brown, D. L. 1978. Freezing point depression of aqueous sodium chloride solutions. *Econ. Geol.* **73**, 284–285.

Price, C. A. 1986. Geology of the Iveragh Peninsula incorporating a remote sensing lineament study. Unpublished Ph.D. thesis, University of Dublin.

Price, C. A. & Todd, S. P. 1988. A model for the development of the Irish Variscides. *J. geol. Soc. Lond.* **145**, 935–939.

Price, N. J. & Cosgrove, J. W. 1990. *The Analysis of Geological Structures*. Cambridge University Press, Cambridge.

Ramberg, H. 1955. Natural and experimental boudinage and pinch-and-swell structures. *J. Geol.* **63**, 512–26.

Ramsay, J. G. 1980. The crack-seal mechanism of rock deformation. *Nature* **284**, 135–139.

Ramsay, J. G. & Huber, M. I. 1987. *The Techniques of Modern Structural Geology, Volume 2: Folds and Fractures*. Academic Press, London.

Roedder, E. 1984. Fluid inclusions (edited by Ribbe, H. P.). *Rev. Miner.* **12**.

Sanderson, D. J. 1984. Structural variation across the northern margin of the Variscides in NW Europe. In: *Variscan Tectonics of The North Atlantic Region* (edited by Hutton, D. H. & Sanderson, D. J.). *Spec. Publ. geol. Soc. Lond.* **14**, 149–165.

Secor, D. T. 1965. Role of fluid pressure in jointing. *Am. J. Sci.* **263**, 633–646.

Shepherd, T. J., Rankin, A. H. & Alderton, D. H. 1985. *A Practical Guide to Fluid Inclusion Studies*. Blackie & Son Ltd., Glasgow.

Sheridan, D. J. 1964. The structure and mineralisation of the Mountain Mine Area, Allihies, West Cork, Ireland. *Scient. Proc. R. publ. Soc.* **A2**, 21–27.

Shimamoto, T., Kanori, Y. & Asai, K.-I. 1991. Cathodoluminescence observations on low-temperature mylonites: potential for detection of solution-precipitation microstructures. *J. Struct. Geol.* **8**, 967–973.

Sibson, R. H. 1985. A note on fault reactivation. *J. Struct. Geol.* **7**, 751–754.

Sibson, R. H. 1988. High-angle reverse faults, fluid pressure cycling and mesothermal gold–quartz deposits. *Geology* **16**, 551–555.

Sibson, R. H. 1989. Earthquake faulting as a structural process. *J. Struct. Geol.* **11**, 1–14.

Sibson, R. H. 1993. Crustal stress, faulting and fluid flow. *Geofluids 1993 Extended Abstracts*, 137–140.

Slater, D. J., Yardley, B. W. D., Spiro, B. & Knipe, R. J. In press. Incipient metamorphism and deformation in the Variscides of SW Dyfed, Wales: first steps towards isotopic equillibrium. *J. metamorphic Geol.*

Sprunt, E. S. & Nur, A. 1979. Microcracking and healing in granite: new evidence from cathodoluminescence. *Science, N.Y.* **205**, 495–497.

Stephenson, O. & Berner, H. 1971. The finite element method in tectonic processes. *Phys. Earth & Planet Interiors* **4**, 310–321.

Stromgard, K. E. 1973. Stress distribution during formation of boudinage and pressure shadows. *Tectonophysics* **16**, 215–248.

Summers, J. M. 1979. An experimental and theoretical investigation of multilayer fold development. Unpublished Ph.D. thesis, University of London.

Voight, B. 1965. Plane flow of viscous matrix with an internal layer compressed between two rectangular, parallel rigid plates. A geological application and a potential viscometer in distorted rocks. *Bull. geol. Soc. Am.* **52**, 1355–1418.

Vrolijk, P. 1987. Tectonically driven fluid flow in the Kodiak accretionary complex, Alaska. *Geology* **15**, 466–469.

Walter, J. V. & Helgeson, H. C. 1977. Calculation of the thermodynamic properties of aqueous silica and the solubility of quartz and its polymorphs at high pressures and temperatures. *Am. J. Sci.* **277**, 1315–1351.

Williams, E. A., Bamford, M. L. F., Cooper, M. A., Edwards, H. E., Ford, M., Grant, G. G., MacCarthy, I. A. J., McAfee, A. M. & O'Sullivan, M. J. 1989. Tectonic controls and sedimentary response in the Devonian–Carboniferous Munster and South Munster basins, southwest Ireland. In: *Role of Tectonics in Devonian and Carboniferous Sedimentation in the British Isles* (edited by Arthurson, R. S., Gutteridge, P. & Nolan, S. C.). *Spec. Publ. York. geol. Soc.* **6**, 123–141.